Protonation of Phosphoramide Mustard and Other Phosphoramides

Michael P. Gamcsik,*,† Susan M. Ludeman,‡ Ellen M. Shulman-Roskes,‡ Ian J. McLennan,§ Michael E. Colvin,⊥ and O. Michael Colvin‡

The Department of Radiology and The Oncology Center, The Johns Hopkins University School of Medicine, Baltimore, Maryland 21205, the Department of Chemistry, Dalhousie University, Halifax, Nova Scotia B3H 4J3, Canada, and the Center for Computational Engineering, Sandia National Laboratories, Livermore, California 94551

Received June 21, 1993•

The chemistry of the bifunctional alkylating agent phosphoramide mustard and model phosphoramides was probed by multinuclear NMR spectroscopy as a function of pH. Between pH 1 and 11, both the ^{31}P and ^{15}N resonances for phosphoramide mustard displayed a single monobasic titration curve with a pK_a of 4.9. The protonation below pH 4.9 correlates with the loss in reactivity of the mustard. The ^{17}O NMR spectrum of ^{17}O-enriched phosphoramide mustard shows little change with pH. The data on the mustard was compared to ^{15}N and ^{31}P NMR data on ^{15}N-enriched phosphoramidic acid, phosphorodiamidic acid, and phosphoric triamide. Contrary to the conclusions of previous studies, our combined ^{31}P, ^{15}N, and ^{17}O NMR results are more consistent with N-protonation of phosphoramide mustard rather than an O-protonation. Theoretical calculations on the phosphoramidic acid, phosphorodiamidic acid, and phosphoric triamide show O-protonation to be more stable in the gas phase. For the latter two compounds, the calculations suggest that N-protonation may be the most stable protonated form in the aqueous phase. These findings influence our understanding of the structure–activity relationships of phosphoramide mustards.

Introduction

Phosphoramide mustard is a bifunctional alkylating agent produced *in vivo* as a metabolite of the widely used anticancer drug cyclophosphamide.[1] The cytotoxic action of phosphoramide mustard is thought to be a result of the formation of interstrand cross-links between deoxyguanosine residues of DNA.[2,3] The high therapeutic index of cyclophosphamide, and related drugs such as ifosfamide, has spurred interest in understanding the chemistry of these alkylating agents. Understanding the factors in molecular structure which influence the chemical reactivity is paramount to the development of new, more effective drugs.

Previous studies of phosphoramide mustard have concluded that, at neutral pH, the drugs exists as a monoanion (1). A reduction in pH has reportedly resulted in protonation of the oxygen to a neutral species (2) with a pK_a between 4.6 and 4.8.[4-7] The site of protonation has been assumed to be the oxygen atom, although two titratable nitrogen atoms are nearby (i.e. structures 3 and 4; Scheme I).

Lowering the pH below 7.4 decreases the reactivity of phosphoramide mustard.[6] This was thought to be due to the loss of the formal negative charge at oxygen since the parent drug cyclophosphamide[1,8] and O-esters of phosphoramide mustard[6,8] have low reactivities.

Phosphoramide mustard alkylates DNA via a two-step mechanism. The sequence is initiated by the nucleophilic displacement of chloride by the bis(chloroethyl)amine nitrogen (i.e. N^2)[9] to form the reactive aziridinium ion. The formation and reactivity of this aziridinium ion toward the N^7 position of guanosine would generally be expected to be related to the basicity of the parent amine. Determining the site of protonation is, therefore, important in understanding the chemistry and reactivity of phosphoramide mustards.

Scheme I

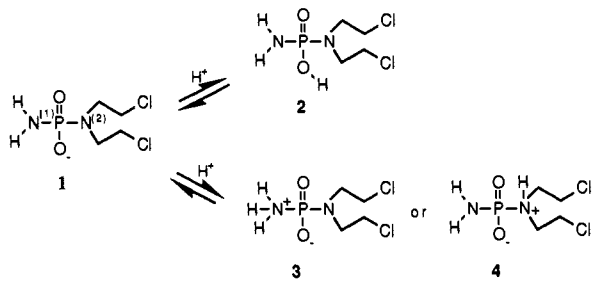

Our laboratory recently reported the syntheses of phosphoramide mustards labeled with ^{15}N and ^{17}O stable isotopes.[10] In addition, the syntheses of three model compounds, [^{15}N]phosphoramidic acid (5), [^{15}N]phosphorodiamidic acid (6), and [^{15}N]phosphoric triamide (7) are reported herein. Using the labeled mustards and these model compounds, we have acquired their ^{15}N, ^{17}O, and ^{31}P NMR spectra as a function of pH. A plot of the ^{31}P and ^{15}N chemical shifts of phosphoramide mustard versus pH can be fit to a single sigmoid curve between pH 1 and 11 with a pK_a of 4.9. However, the direction and magnitude of the changes in chemical shifts are more consistent with protonation of the N^1 nitrogen of phosphoramide mustard rather than with that of the oxygen. Thus, below pH 4.9, the predominant solution structure of phosphoramide mustard is a zwitterion (3) rather than an uncharged species.

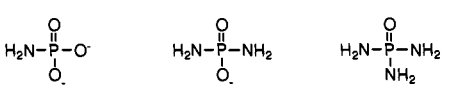

* Address correspondence to this author at Division of NMR Research, 340 Traylor Building, 720 Rutland Ave, Baltimore, MD 21205.
† Department of Radiology, The Johns Hopkins University School of Medicine.
‡ Oncology Center, The Johns Hopkins University School of Medicine.
§ Dalhousie University.
⊥ Sandia National Laboratories.
• Abstract published in *Advance ACS Abstracts*, October 15, 1993.

0022-2623/93/1836-3636$04.00/0

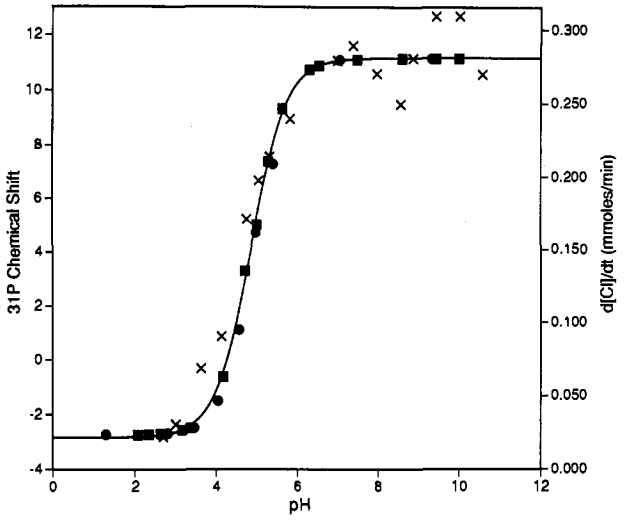

Figure 1. The ^{31}P chemical shifts of [$^{15}N^1$]phosphoramide mustard (squares) and [$^{15}N^2$]phosphoramide mustard (circles) as a function of pH at 4 °C. A single sigmoid curve was fit to the data with a pK_a of 4.85 ± 0.01. The rate of chloride ion production (crosses) as a function of pH at 20 °C. A single sigmoid curve was fit to this data with a pK_a of 4.72 ± 0.03 (curve not shown for clarity). Errors given are for the least squares curve fit.

Results and Discussion

Phosphoramide Mustard. ^{31}P NMR Studies. The ^{31}P NMR chemical shift of phosphoramide mustard as a function of pH at 4 °C is shown in Figure 1. The data was obtained at low temperature in order to slow P–N bond hydrolysis, which occurs below pH 4.5.[5,6,11] The reduced temperature allowed study of the NMR parameters over a wider pH range than previously reported.[5,6] Curve fitting of the data presented in Figure 1 with a single sigmoid function resulted in a calculated pK_a of 4.9. This agreed with the value of 4.75 (at 20 °C) determined in previous ^{31}P NMR studies[6] and with the values of 4.8 (at 0 °C)[7] and 4.7[4] determined using other methods. Theoretical calculations[12] predicted a pK_a of 4.58. In each of the previous studies, it was assumed that this pK_a value corresponded to protonation of the oxygen.

The analysis of the ^{31}P NMR data alone cannot discriminate between oxygen and nitrogen protonation. Since the phosphorus atom in phosphoramide mustard is one bond removed from any protonation site (either oxygen or nitrogen), relating ^{31}P chemical shift changes directly to a particular site is difficult.[13] On the other hand, it can be noted that the behavior of the ^{31}P shift of phosphoramide mustard as a function of pH is not similar to that found for phosphate groups where O-protonation occurs. The 14.0 ppm upfield shift in the ^{31}P NMR resonance which occurs upon protonation (Figure 1) is unusual in that it is much larger than that normally found for protonation of phosphate groups (Table I). For example, the ^{31}P NMR spectrum of inorganic phosphate shifted upfield by 0.2, 2.3, and 2.5 ppm for protonations at pK_a 2, 6.8, and 11.5, respectively.[14] One of the largest shifts observed for a protonation of a phosphate group was the 4.7 ppm upfield shift observed for the γ-phosphorus of ATP[14] (Table I).

Protonation of phosphoramide mustard profoundly affects its reactivity. Formation of the reactive aziridinium ion of phosphoramide mustard occurs through the displacement of a chlorine atom by the N^2 nitrogen. As a measure of reactivity, the rate of chloride ion liberation was determined as a function of pH for phosphoramide mustard at 20 °C using a chloride ion specific electrode. The rate of chloride ion release and hence, chemical reactivity, is dependent upon a protonation process that occurs with a pK_a of 4.7 (Figure 1). The pK_a of 4.7 closely corresponds to the pK_a of 4.75 previously deterined by ^{31}P NMR at 20 °C.[6] Both values reflect a difference in pK_a with temperature when compared to the determination (pK_a = 4.9) at 4 °C. The temperature dependence of protonation is similar to that observed with model phosphoramides (*vide infra*). These results demonstrate that the protonation of phosphoramide mustard is closely linked to its reactivity. Therefore, by determining the site of protonation in phosphoramide mustard, we will begin to understand some of the factors which directly affect reactivity of alkylating nitrogen mustards.

Table I. ^{31}P Chemical Shift Changes Due to Protonation

compound	Δ shift[a] (ppm)	pK_a	ref
inorganic phosphate	−2.7	11.8	14
	−2.5	6.7	14
	−0.2	2.0	14
ATP (γ-P)	−4.7	6.6	14
methylphosphonate $CH_3PO_3^{2-}$	3.9	7.6	19
imidodiphosphate (PNP) $HN(PO_3^{2-})_2$	−0.2	10.3	20
	−1.9	7.4	20
imidodiphosphate tetramethyl ester $HN(PO(OC_2H_5)_2)_2$	−1.2	3.8	20
AMP-PNP (β-P)	−3.3	8.2	20
(γ-P)	−1.1	8.3	20
phosphoramide mustard	−14.0	4.9	this work
phosphoramidic acid (5)	−3.2	3.0	this work
	−12.0	8.3	this work
phosphorodiamidic acid (6)	−14.2	5.4	this work

[a] Upfield shifts are negative, downfield are positive, with decreasing pH.

In order to obtain more direct evidence for the specific site(s) of protonation, the nitrogens and oxygens of phosphoramide mustard were enriched with NMR-detectable isotopes. Both [^{15}N]- and [^{17}O]phosphoramide mustards were prepared by published methods.[10]

^{15}N NMR Studies. The pH dependencies of the ^{15}N chemical shifts of phosphoramide mustards separately labeled at the N^1 and N^2 positions are shown in Figure 2. At 4 °C, both resonances titrate with a single pK_a of 4.9. The resonance from N^1-labeled phosphoramide mustard shows a downfield shift of 12.7 ppm with protonation whereas the resonance from the N^2-labeled compound shifts 0.4 ppm in the opposite direction. The downfield shift of 12.7 ppm for the ^{15}N resonance of N^1-labeled phosphoramide mustard is typical of shifts observed for the protonation of alkylamine groups[15] and thus is consistent with protonation of phosphoramide mustard at N^1 (Table II).

The proton-coupled ^{15}N NMR spectrum of the N^1-labeled compound shows a multiplicity change with variations in pH which is indicative of a change in proton exchange rates (Figure 3). At high pH, a doublet of triplets is observed due to the one-bond scalar coupling to the two attached protons ($^1J(^{15}N–^1H)$ = 73.6 Hz) and the one phosphorus atom ($^1J(^{15}N–^{31}P)$ = 17.2 Hz; Figure 3e). As the pH is lowered, this resonance broadens, then narrows to a doublet ($^1J(^{15}N–^{31}P)$ = 14.1 Hz) near pH 5.5 (Figure 3c), broadens again, and finally narrows to a doublet with a smaller coupling constant ($^1J(^{15}N–^{31}P)$ = 3.1 Hz; Figure 3a). Although the changes in $^{15}N–^1H$ coupling only reflect

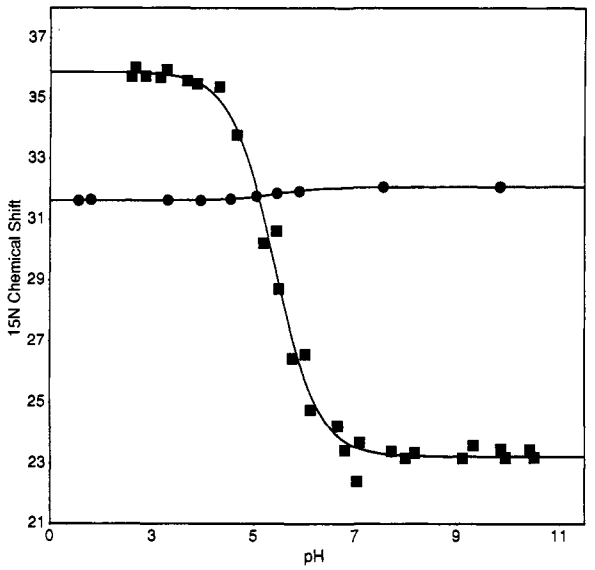

Figure 2. The ^{15}N chemical shift of [$^{15}N^1$]phosphoramide mustard (squares) and [$^{15}N^2$]phosphoramide mustard (circles) as a function of pH at 4 °C. In each case a sigmoid curve was fit to the data. For $^{15}N^1$, $pK_a = 4.91 \pm 0.04$; for $^{15}N^2$, $pK_a = 4.95 \pm 0.01$.

Table II. ^{15}N Chemical Shift Changes Due to Protonation

compound	Δ shift[a] (ppm)	pK_a	ref
methylamine	15.9	nd[b]	15[c]
ethylamine	8.7	nd	15
propylamine	10.6	nd	15
dimethylamine	12.9	nd	15
diethylamine	3.6	nd	15
trimethylamine	13.4	nd	15
imidazole	−31.0	7.0	50
histidine $N\tau$	−5.0	6.2	51
$N\pi$	−55.9	6.2	51
imidodiphosphate (PNP) $HN(PO_3^{2-})_2$	−3.4	nd	20
imidodiphosphate tetraethyl ester $HN(PO(OC_2H_5)_2)_2$	−2.5	nd	20
AMP-PNP	≥−1.1	nd	20
phosphoramidic acid (5)	1.2	2.8	this work
	6.3	8.2	this work
phosphorodiamidic acid (6)	3.6	5.4	this work
[$^{15}N^1$]phosphoramide mustard	12.7	4.9	this work
[$^{15}N^2$]phosphoramide mustard	−0.4	4.9	this work

[a] Upfield shifts are negative, downfield are positive, with decreasing pH. [b] Not determined from ^{15}N data. [c] Alkylamine protonation shifts determined in methanol.[15]

a change in exchange rates for the protons, this data, as well as the magnitude and direction of the chemical shift changes (*vide supra*), are all consistent with protonation occurring at the N^1 nitrogen of phosphoramide mustard.

^{13}C NMR Studies. The natural abundance ^{13}C NMR spectrum of unlabeled phosphoramide mustard was obtained as a function of pH at 4 °C. Both carbon resonances exhibited monobasic titration behavior with a pK_a value of 4.9 (data not shown). The resonance from the α-carbon atom, adjacent to the N^2, shifted upfield 1.53 ppm upon protonation whereas the resonance from the β-carbon atom shifted upfield by 0.72 ppm. Usually, protonation of an amine causes a larger upfield shift in the resonance of the β-carbon than the resonance of the directly bonded α-carbon, the so-called "β-effect".[16] The lack of a "β-effect" on the carbon resonances argues against, but does not entirely rule out, the protonation of the N^2 nitrogen below pH 4.9. Protonation of the N^1 nitrogen is consistent with these results since the shifts in the ^{13}C spectrum for carbons

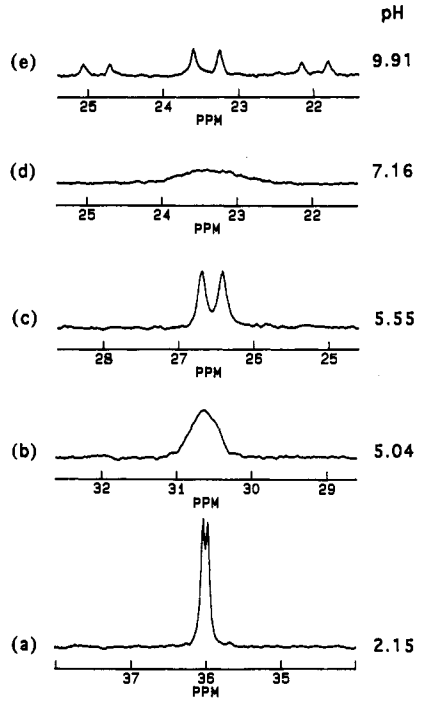

Figure 3. The proton-coupled ^{15}N NMR spectra of [$^{15}N^1$]-phosphoramide mustard in 0.2 M NaCl, 10% D_2O at the indicated pH at 4 °C.

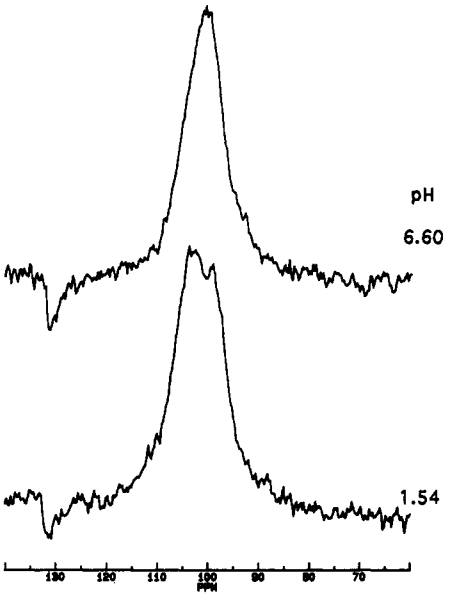

Figure 4. The ^{17}O NMR spectra of [^{17}O]phosphoramide mustard in 0.2 M NaCl, 90% H_2O/10% D_2O at the indicated pH at 4 °C.

three and four bonds away from the titrating nitrogen decrease with the number of intervening bonds.

^{17}O NMR Studies. The ^{17}O NMR spectrum of ^{17}O-labeled phosphoramide mustard is shown in Figure 4. Due to the predominance of the quadrupolar relaxation mechanism for ^{17}O and the fact that the experiment needed to be performed at low temperature (for the increased stability of the mustard), the NMR line shape is broad and obscures any heteronuclear scalar coupling. Between pH 4 and 12, the ^{17}O resonance shows little or no change. As the pH is lowered below 4, the line shape changes and the position may shift slightly, although the error in the determination of the chemical shift of the broad resonances is as large as the possible change in shift (see Figure 4). As a comparison to other compounds, the ^{17}O resonance

Table III. ^{17}O Chemical Shift Changes Due to Protonation

compound	Δ shift[a] (ppm)	pK_a	ref
sodium phosphate	-6.6		17
	-12.3		17
	-12.3		17
[γ-^{17}O]ATP	-15.6	6.9	18
imidodiphosphate (PNP) $HN(PO_3^{2-})_2$	-9.6	10.4	20
	-8.8	7.4	20
imidodiphosphate tetraethyl ester $N(PO(OC_2H_5)_2)_2$	-5.4[b]	4.2	20
AMP-PNP	-15.6	8.2	20
phosphoramide mustard	~0		this work

[a] Upfield shifts are negative, downfield are positive, with decreasing pH. [b] Shift associated with N-protonation.[20]

of sodium phosphate shifts upfield 12.3, 12.3, and 6.6 ppm as the compound undergoes sequential protonation at the three titratable oxygens[17] (Table III). Similarly, during the titration of a series of phosphates and phosphonates, upfield shifts between 8 and 24 ppm are observed for the ^{17}O resonances[18,19] (Table III). Reynolds *et al.*[20] report shifts between 9 and 14 ppm upfield for O-protonation in two imidodiphosphates studied by ^{17}O NMR. A smaller ^{17}O shift (5 ppm upfield) is reported for an imidodiphosphate in which N-protonation occurs[20] (Table III). The lack of change in the ^{17}O chemical shift of phosphoramide mustard with pH is unlike the large shifts observed with O-protonation of other compounds.

The presence of an intramolecular hydrogen bond formed between a protonated N^1 and oxygen (i.e. a structure between **2** and **3**) also appears to be unlikely due to the fact that no pH-induced change is observed in the ^{17}O chemical shifts of phosphoramide mustard. The ^{17}O chemical shift is usually sensitive to the presence of hydrogen bonding.[21]

Other Phosphoramides. Although comparisons of our ^{31}P, ^{15}N, and ^{17}O phosphoramide mustard data to previous studies on amines, phosphates, phosphonates, and imidodiphosphates were consistent with N^1-protonation, we sought to study compounds which more closely modeled the chemistry found with phosphoramide mustard. Therefore, a series of ^{15}N-labeled phosphoramides were synthesized and studied by ^{15}N and ^{31}P NMR.

^{31}P NMR Studies. The compound [^{15}N]phosphoric triamide (**7**) was synthesized as outlined in the Experimental Section. The major impurity found in this preparation was [^{15}N]phosphorodiamidic acid (**6**). Since this compound also served as a model for phosphoramide mustard, these preparations were used without further purification. At low pH, an aqueous solution of these compounds hydrolyzed to [^{15}N]phosphoramidic acid (**5**), which was also included in the study. For phosphorodiamidic acid and phosphoramidic acid, the protonation sites have been determined previously by other methods.[22-24] The ^{31}P NMR shifts for these three compounds were plotted as a function of pH as shown in Figure 5.

The ^{31}P chemical shift for the phosphoric triamide was insensitive to pH (Figure 5). However, below pH 4, rapid hydrolysis of the triamide occurred even at 4 °C. Phosphorodiamidic acid underwent slower hydrolysis at low pH, which allowed time for observation by NMR below pH 4. The ^{31}P NMR spectrum for this diamidate displayed a monobasic change in chemical shift with decreasing pH (pK_a of 5.4) (Figure 5). The 14.2 ppm upfield shift upon protonation was similar to that observed with phosphoramide mustard and, by the same arguments presented above, suggested N-protonation. The pK_a of phosphorodiamidic acid was previously reported to be 4.9 at 25 °C; however, the authors did not specify whether this value was associated with N- or O-protonation.[22] On the other hand, Rahil and Haake[23] implied that the pK_a of 4.9 was due to protonation of one of the nitrogens. Our NMR data supports this conclusion. The variance in pK_a values (5.4 versus 4.9) may be due to experimental differences in both temperature and ionic strength (*vide infra*).

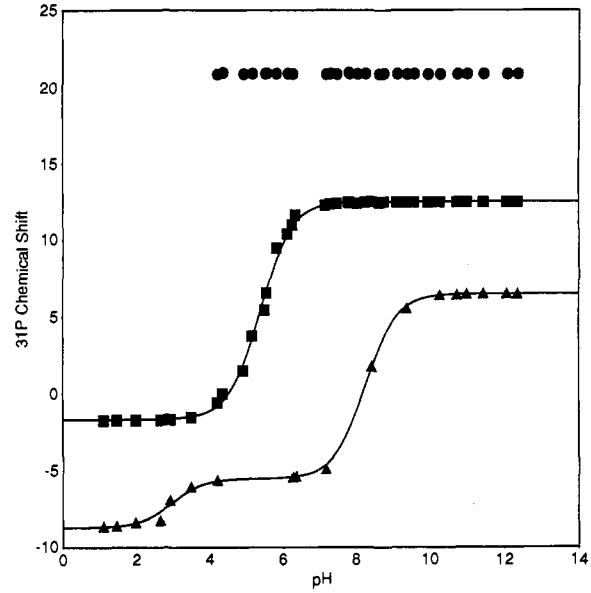

Figure 5. The ^{31}P chemical shifts for phosphoric triamide (**7**) (circles), phosphorodiamidic acid (**6**) (squares), and phosphoramidic acid (**5**) (triangles) as a function of pH at 4 °C. The data for **6** was fit to a single sigmoid curve, yielding a $pK_a = 5.38 \pm 0.02$. The data for **5** was fit to a double sigmoid with $pK_{a1} = 2.96 \pm 0.04$ and $pK_{a2} = 8.25 \pm 0.04$.

Scheme II

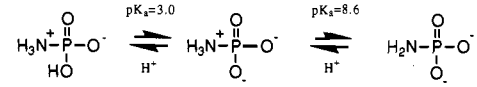

The ^{31}P NMR data as a function of pH for phosphoramidic acid (**5**) exhibits a biphasic curve with pK_a values of 3.0 and 8.3 (Figure 5). The lower pK_a is associated with a small upfield shift of 3.2 ppm. The magnitude and direction of this shift is consistent with O-protonation (Table I). The larger upfield shift of 12.0 ppm ($pK_a = 8.3$) is similar to that observed for phosphorodiamidic acid (**6**) and for phosphoramide mustard. This is consistent with N-protonation because shifts observed with O-protonation are usually much smaller (Table I). From second ionization enthalpies, a previous study concludes that their observed pK_a of 8.6 for phosphoramidic acid is characteristic of N-protonation and that protonation of one of the oxygens occurs with a pK_a value of 3.0[24] (Scheme II). The ^{31}P NMR results presented herein are entirely consistent with these conclusions. The ionization enthalpy of N-protonation of phosphoramidic acid indicates that the pK_a is sensitive to temperature and ionic strength.[24] For phosphoramidic acid, the pK_a for N-protonation increases with decreasing temperature and decreases with increasing ionic strength. The reported values in Scheme II refer to values at 25 °C, extrapolated to infinite dilution. Therefore, the slight differences in the pK_a values determined in this report, relative to previously published values, may be due to both temperature and ionic strength effects. Similar

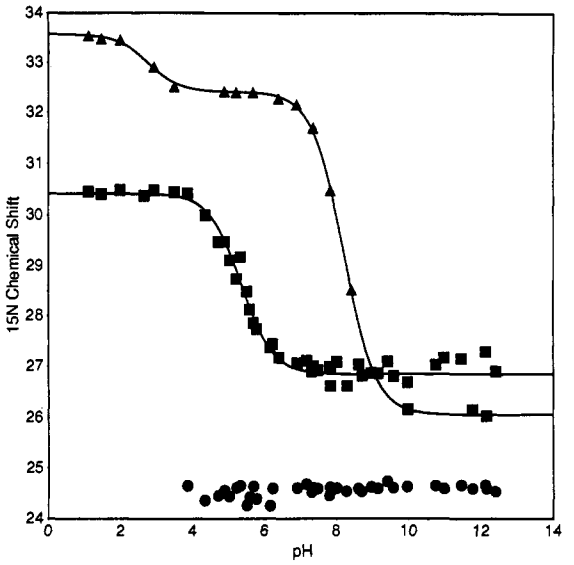

Figure 6. The ^{15}N chemical shifts for phosphoric triamide (7) (circles), phosphorodiamidic acid (6) (squares), and phosphoramidic acid (5) (triangles) as a function of pH at 4 °C. The data for 6 was fit to a single sigmoid curve, yielding a pK_a = 5.35 ± 0.01. The data for 5 was fit to a double sigmoid with pK_{a1} = 2.82 ± 0.03 and pK_{a2} = 8.20 ± 0.03.

temperature dependent effects on the pK_a of phosphoramide mustard have also been observed (Figure 1).

The ^{31}P data are summarized in Table I. The data for phosphoramidic acid (5) demonstrate the relative contribution of N- vs O-protonation to the chemical shift of the attached ^{31}P nucleus. The change in chemical shift of the ^{31}P resonance due to N-protonation is larger than the change in chemical shift of the ^{31}P resonance caused by O-protonation. This supports our conclusion for N-protonation in phosphoramide mustard since a similar change in chemical shift (14.0 ppm) is observed for this compound (Table I). Differences in the change in chemical shift of the ^{15}N resonance between N- and O-protonation can be observed by ^{15}N NMR (*vide infra*).

^{15}N NMR Studies. Figure 6 shows the dependence of the ^{15}N chemical shift on pH for the three model compounds (5–7). As found for the ^{31}P signal, the chemical shift of the ^{15}N resonances of the triamide (7) shows no change over the titratable range. In the proton-coupled ^{15}N spectrum, however, the multiplicity of the ^{15}N resonances for the triamide changes (Figure 7). Above pH 11.5, a doublet is observed ($^1J(^{15}N-^{31}P)$ = 21.9 Hz). Between pH 7 and 10 a doublet of triplets is detected ($^1J(^{15}N-^{31}P)$ = 21.9 Hz; $^1J(^{15}N-^1H)$ = 87.0 Hz); this collapses to a doublet below pH 6 ($^1J(^{15}N-^{31}P)$ = 22.3 Hz). Although no change in chemical shift is observed in either the ^{31}P or ^{15}N NMR spectrum, the variation in coupling patterns indicates that the exchange rates for the protons of the triamide are pH dependent.

The ^{15}N NMR spectrum of the diamidate (6) shifts 3.6 ppm to low-field with a reduction in pH. This shift is smaller than that found for phosphoramide mustard but is not unusual for the protonation of some alkylamines (Table II). Both ^{31}P and ^{15}N data result in a pK_a determination of 5.4 for the diamidate. The proton-coupled ^{15}N NMR spectra show similar behavior to those seen with phosphoramide mustard. Between pH 10.5 and 12, a doublet of triplets ($^1J(^{15}N-^{31}P)$ = 15.7 Hz; $^1J(^{15}N-^1H)$ = 72.8 Hz) is observed which broadens and appears as a doublet ($^1J(^{15}N-^{31}P)$ = 15.7 Hz) below pH 8.5 (Figure 7). Unlike phosphoramide mustard (Figure 3a,c), the coupling of the doublet does not change as the pH is lowered further.

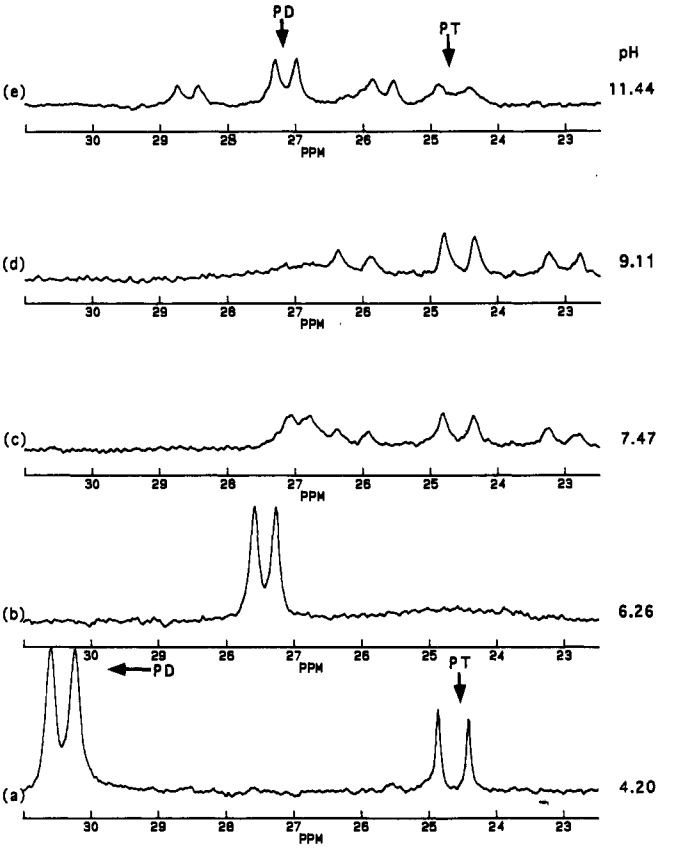

Figure 7. The ^{15}N NMR spectra for phosphorodiamidic acid (PD) and phosphoric triamide (PT) in 0.2 M NaCl, 10% D_2O at the indicated pH at 4 °C.

The titration curve for the phosphoramidic acid (5) resonance displays dibasic behavior with a small 1.2 ppm downfield shift (pK_a 2.8) and a larger 6.3 ppm downfield shift (pK_a 8.2). The changes in the ^{15}N spectrum with pH indicate that the smaller ionization shift correlates with O-protonation and the larger shift can be attributed to N-protonation. These results are consistent with the ^{31}P data. The proton-coupled ^{15}N NMR spectrum of the phosphoramidic acid is a doublet with a small $^{15}N-^{31}P$ coupling constant ($^1J(^{15}N-^{31}P)$ = 2.5 Hz) up to pH 8. This indicates a rapid exchange of the attached protons of the amide group (data not shown). Above this pH, the resonance broadens to obscure any heteronuclear scalar coupling. The ^{15}N data are summarized in Table II.

The finding that phosphoramide mustard undergoes N-protonation at low pH is not unique for phosphoramides as a group. Studies of other phosphoramides have presented arguments for both N- and O-protonation. There is ample experimental evidence for the N-protonation of phosphoramidic acid (5) to produce the zwitterion.[24-26] Other phosphoramides[27] such as $(NMe_2)_2PO_2H$, $NEt_2PO(OEt)OH$, and a series of phenylphosphonamides[23] undergo N-protonation to form the zwitterionic species.

Theoretical Studies. Bollinger *et al.*[28] reported gas-phase basicities for a series of phosphine oxides and phosphoramides and concluded that O-protonation was predominant. This experimental data was supported by *ab initio* results which indicated that O-protonation was favored over N-protonation by ca. 100 kcal/mol. These authors suggested that the experimental gas-phase results

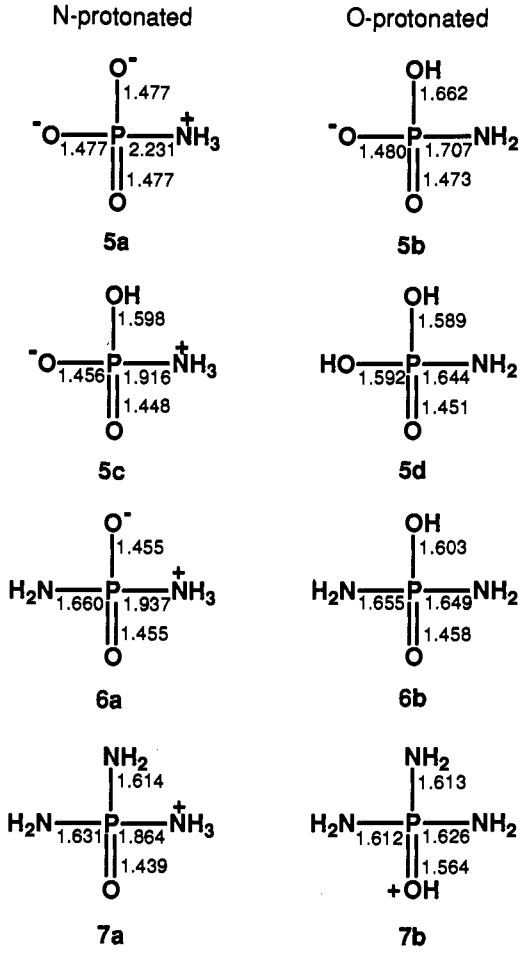

Figure 8. Structures of N- and O-protonated phosphoramidic acid, phosphorodiamidic acid, and phosphoric triamide. The numbers shown are the 6-31G* HF-optimized bond lengths. All distances are in angstroms. Bond orders and charge locations are approximate.

could be directly extrapolated to the condensed phase; however, no solution phase experimental or theoretical data were presented. Gas-phase *ab initio* calculations on the phosphinamide $H_2P(O)NH_2$ also concluded that O-protonation was more stable than N-protonation.[29] However, direct extrapolation of relative stabilities from the gas phase to solution phase may not be straightforward. In order to place our experimental results in a similar context, *ab initio* calculations on the O- and N-protonated model phosphoramides (**5a–d, 6a,b, 7a,b**) were performed both in the gas phase and in the aqueous phase.

The 6-31G* Hartree-Fock (HF) optimized bond lengths are shown in Figure 8. The 6-31G*-optimized structures yielded bond lengths for the neutral species in good agreement with experimental values[30] determined for P=O (1.45–1.46 Å), P—OH (1.59–1.60 Å), and P—NH_2 (1.64–1.67 Å). Protonation of the nitrogen atoms led to much longer P–NH_3^+ bonds of 1.92–2.23 Å. The reoptimization of the anionic phosphoramidic acids with the larger basis set had only minor effects, with most bond lengths changing by less than 0.01 Å. The exception to this was the very elongated P–N bond in the N-protonated form (**5a**) which increased from 2.23 to 2.28 Å with the larger basis set.

The gas-phase second-order (MP2) and single-point fourth-order (MP4) Møller–Plesset perturbation theory energies as well as the HF vibrational zero point energies are given for the phosphoramides in Table IV. The data

Table IV. Gas-Phase Energies of N- and O-Protonated Phosphoramidic Acids[a]

species	zero-point energy[b] (kcal/mol)	E_{MP4} (6-31G**) (hartrees)	ΔE^c (kcal/mol)	E_{MP2} (6-311++G**) (Hartrees)	ΔE^c (kcal/mol)
5a	33.7	−622.483 118	−16.9	−622.640 501	−16.8
5b	33.8	−622.510 178		−622.667 513	
5a[d]	33.7	–	–	−622.639 784	−16.6
5b[d]	33.8	–	–	−622.666 393	
5c	43.3	−623.053 956	−13.5	−623.188 856	−14.8
5d	41.3	−623.072 236		−623.209 305	
6a	51.5	−603.215 429	−11.9	−603.329 611	−12.3
6b	50.0	−603.232 111		−603.346 893	
7a	67.2	−583.742 527	−12.3	−583.822 596	−13.5
7b	65.8	−583.759 918		−583.841 916	

[a] Except where indicated, all structures optimized at the HF level of theory using a 6-31G* basis set. [b] The zero-point energies was calculated from the HF 6-31G* harmonic vibrational frequencies. [c] Energy difference = (N-protonated minus O-protonated), includes zero-point energies. [d] Structure optimized using 6-311++G** basis set.

in Table IV predict the O-protonated forms to be more stable than the N-protonated forms by 12–17 kcal/mol. The MP2/6-311++G** and the MP4/6-31G** relative O- versus N-protonation energies were in very good agreement (within 1.3 kcal/mol) for all species, indicating that the diffuse basis functions were not essential to describe these zwitterionic and anionic species. Reoptimization of the anionic phosphoramidic acids (**5a,b**) had almost no effect on the relative energies of the protonated species, changing by only 0.2 kcal/mol.

It is not surprising that the O-protonated forms are predicted to be more stable in the gas phase. These compounds are analogous to the amino acids, where the neutral O-protonated form is the most stable in the gas phase and the N-protonated zwitterionic form, involving a large charge separation, is more stable in polar solvents.[31,32] This analogy is clear for the neutral and zwitterionic phosphoramidic acid (**5c**) and phosphorodiamidic acid (**6a**), but is less so for the anionic phosphoramidic acid (**5a**) and the cationic phosphoric triamides (**7a,b**). The Mulliken populations given in Table V indicate that there is a much larger charge separation in the N-protonated form than the O-protonated form for all species. This indicates that the "neutral-zwitterion" analogy is indeed reasonable for understanding the preference of O-protonation in the gas phase (with the possible exception of the anionic phosphoramidic acid species described below).

The components of the aqueous solvation energy and the total aqueous phase energy ($E_{MP4} + E_{solv} - ZPE$) are given in Table VI. Two sets of results are given for the anionic phosphoramidic acid spcies (**5a,b**) in order to compare the energies for the 6-31G*- and 6-311++G** HF-optimized structures. Only the MP2 energy was calculated for the 6-311++G**-optimized structures. The cavitation term, ΔG_{cav} (the energy required to form a "solute-sized" cavity in water), is essentially constant for all species since they have nearly identical molecular volumes and surface areas. The values of the total solvation free energies are in good agreement with experiment and other theory in finding ΔG_{solv} of −15 to −20 kcal/mol for neutral, highly polar molecules an ΔG_{solv} of −80 to −105 kcal/mol for cations and anions.[33–35] In all species studied here, the N-protonated zwitterionic form has a much more negative solvation free energy than the corresponding O-protonated form. Except for species **5a**

Table V. Mulliken Populations of N- and O-Protonated Phosphoramidic Acids[a]

species	Mulliken populations		
	phosphorus	nitrogen	oxygen
5a	1.43	0.07	−0.83 (−O)
			−0.83 (−O)
			−0.83 (−O)
5b	1.45	−0.34	−0.45 (OH)
			−0.81 (−O)
			−0.85 (−O)
5c	1.52	0.27	−0.33 (OH)
			−0.71 (−O)
			−0.74 (−O)
5d	1.51	−0.20	−0.30 (OH)
			−0.31 (OH)
			−0.71 (=O)
6a	1.49	−0.25 (NH_2)	−0.74 (−O)
		0.25 (NH_3)	−0.74 (−O)
6b	1.47	−0.21 (NH_2)	−0.32 (OH)
		−0.21 (NH_2)	−0.72 (−O)
7a	1.54	−0.15 (NH_2)	−0.62 (−O)
		−0.13 (NH_2)	
		0.36 (NH_3)	
7b	1.52	−0.12 (NH_2)	−0.23 (OH)
		−0.09 (NH_2)	
		−0.09 (NH_2)	

[a] Mulliken populations with hydrogen charges summed onto the heavy atoms calculated with a 6-31G** basis set at the 6-31G* HF optimized geometries. Where necessary, the specific atom type is indicated after the charge. All charges in atomic units.

Table VI. Aqueous Solvation Energies of N- and O-Protonated Phosphoramidic Acids[a]

structure	ΔG_{cav}[b]	ΔG_{elec}[c]	$\Delta G_s 3o_{lv}$[d]	$\Delta\Delta G_{solv}$[e]	total E_{aq} (hartrees)	ΔE_{aq}[f]
5a	11.1	−115.9	−104.8	11.3	−622.596 515	−5.6
5b	10.7	−104.3	−93.5		−622.605 420	
5a[h]	11.1	−114.0	−103.0	8.4	−622.750 228[i]	−8.2[i]
5b[h]	10.7	−105.3	−94.6		−622.763 310[i]	
5c	11.1	−56.1	−45.0	26.2	−623.056 694	12.8
5d	11.1	−29.8	−18.8		−623.036 323	
6a	11.6	−52.7	−41.0	24.0	−603.198 816	12.1
6b	11.6	−28.6	−17.0		−603.179 544	
7a	12.4	−96.8	−84.4	26.0	−583.769 945	13.7
7b	12.4	−70.7	−58.4		−583.748 128	

[a] All energies in kcal/mol except where otherwise indicated. [b] ΔG_{cav} is the cavitation free energy. [c] ΔG_{elec} is the electrostatic free energy. [d] $\Delta G_{solv} = \Delta G_{cav} + \Delta G_{elec}$ and is the predicted solvation free energy. [e] Difference in ΔG_{solv} for the O-protonated minus the N-protonated forms. [f] The total aqueous phase energy E_{aq} is calculated from the sum of solvation free energy, zero point energy, and MP4 energy (except where indicated). [g] Difference in E_{aq} for N-protonated minus O-protonated forms. [h] Structure optimized using 6-311+G** basis set. [i] Calculated from MP2/6-311++G**.

and **5b**, $\Delta\Delta G_{solv}$ ranges between 24 and 26 kcal/mol. This is close to the best measurements for glycine, which show that the zwitterion has a 29 kcal/mol lower enthalpy of solvation than the neutral form.[31] For the anionic phosphoramidic acids (**5a,b**), $\Delta\Delta G_{solv}$ is only 8.4–11.3 kcal/mol. The reason for this difference is that the N-protonated anionic phosphoramidic acid (**5a**) has a very different structure relative to the other N-protonated species. The predicted gas-phase geometry of this species is nearly dissociated, consisting of a planar PO_3 anion and a neutral NH_3 attached with a very long 2.231-Å "bond". This interpretation is supported by the Mulliken populations (Table V) which show a net charge of −1.07 on the orthophosphate and a +0.07 charge on the amino group. Although this result clearly indicates that in the gas phase the P–N bond in this species is very weak, it is unclear whether this is an accurate picture of the aqueous phase structure of the anionic N-protonated phosphoramide (**5a**). Crystal studies[26] resulted in the determination of a P–N bond length of 1.78 Å for the N-protonated phosphoramidic acid.

The theoretical data indicate that, in the gas phase, the *O*-protonated forms of the model phosphoramides are more stable by at least 11 kcal/mol. In the aqueous phase, the much larger solvation energy of the zwitterionic forms reverses the energy ordering for all species except for the anionic phosphoramidic acid species (**5a,b**). Therefore, for most of these compounds, the nitrogen is predicted to be the preferred protonation site. As described above, the anionic N-protonated phosphoramidic acid (**5a**) has a nearly-dissociated gas-phase structure, raising uncertainty about the prediction that the O-protonated form is preferred.

Both gas-phase and solution-phase *ab initio* data on phosphoramide mustard will be presented in a separate report.[36]

Conclusions

The experimental results of this study suggest that phosphoramide mustard, in solution between pH 1 and 4.9, exists predominately as the zwitterion (**3**). The theoretical data show that N-protonated phosphoramides may be the most stable forms in solution. The experimental evidence appears to rule out structures **2** and **4** as the primary forms of phosphoramide mustard present below pH 4.9. The data do not rule out the possibility of an N^1 protonated form of structure **2**. On the basis of previous studies of the zwitterionic nature of phosphoramidic acid and phosphorodiamidic acid, and the similarities of the NMR spectra of these compounds to phosphoramide mustard, predominance of the zwitterionic structure **3** is favored.

A possible structure for protonated phosphoramide mustard in between that of structures **2** and **3** containing an intramolecular hydrogen bond is not supported by experimental evidence from ^{17}O NMR data nor the theoretical calculations. The calculated structures of phosphoramide mustard and phosphorodiamidic acid show distances between the nitrogen proton and oxygen of between 2.6 and 2.8 Å and an N–H–O angle of nearly 90°. Both factors are not favorable for hydrogen-bond formation.

Protonation of the N^1 in preference to the N^2 suggests that the N^2 of phosphoramide mustard is less able to stabilize a positive charge. Formation of an aziridinium ion occurs via the displacement of a chloride ion and also results in a positive charge localization at the N^2 nitrogen. Although the structure of the protonated mustard (**4**) is different from that of an aziridinium, the inability of the N^2 nitrogen to stabilize a positive charge due to protonation might suggest that an aziridinium ion formed by phosphoramide mustard would be an unstable species. This may be the case since previous studies have not detected the aziridinium of phosphoramide mustard in solution.[11,37] However, the aziridinium ion for mechlorethamine[38,39] and nornitrogen mustard[40] have been observed by NMR in water solution.

The basicity of the nitrogen in phosphoramide mustard and other nitrogen mustards is greatly influenced by its substituents. For example, for mechlorethamine ($CH_3N(CH_2CH_2Cl)_2$; $pK_a = 6.8$), substitution of one chlorine by a hydroxyl group raises the pK_a to 7.8.[41] Substitution of both chlorines by hydroxyl groups raises the pK_a to

8.8.[40] Clearly the inductive effect of the chlorine on the nitrogen atom is reflected in the pK_a. Early experiments have shown that the rates of aziridinium ion formation for related β-chloroethylamines paralleled the basicities of the nitrogens.[41]

The results of this study indicate that the pK_a of the N^2 of phosphoramide mustard is much lower than that of mechlorethamine and therefore must reflect the effect the phosphoramide mustard group has on the nitrogen basicity. The electronic charge of the phosphoramide group, as expected, also influences the activity of the mustard. This is demonstrated by the coincidence of the titration curve and chloride ion release shown in Figure 1. Since the formation of the aziridinium ion is an important prerequisite for DNA cross-linking by nitrogen mustards, understanding the factors which influence the formation and stability of this species is important to predicting the cytotoxic activity of these drugs.

The unique chemistry of the phosphoramide group also influences the stability of the native drug. Earlier reports suggested that at acid pH, P–N bond hydrolysis occurred at room temperature.[6,11] Watson *et al.*[11] suggested that N^2 protonation stabilized the drug below pH 5, but P–N^2 bond hydrolysis was facilitated under more acidic conditions. We are currently investigating the influence of pH on the hydrolysis of both P–N bonds in phosphoramide mustard in order to determine the influence of N^1 protonation on the stability of the drug. These studies are crucial to understanding the pharmacokinetics of phosphoramide mustard in solution.

By developing theoretical models, we hope to predict the influence of a change in structure on the activity and stability of a drug. Critical to developing these theoretical models is the ability to experimentally verify these predicted changes. The measurement of nitrogen basicity of phosphoramides and the correlation with theoretical predictions is the first step in developing models for understanding the structure–activity relationships in phosphoramide mustard.

Experimental Section

Unlabeled Phosphoramide Mustard. Phosphoramide mustard, provided as the cyclohexylammonium salt, was suppplied by the Drug Synthesis and Chemistry Branch, Division of Cancer Treatment, National Cancer Institute.

Labeled Phosphoramide Mustards. [$^{15}N^1$]-, [$^{15}N^2$]-, and [^{17}O]phosphoramide mustards were prepared by published procedures.[10]

Phosphoric Triamide (7). A glass vessel of $^{15}NH_3$ (250-mL break-seal flask, *ca.* 10 mmol, Aldrich Chemical Co., 98 atom % ^{15}N) was wired with a septum and the glass seal was broken. The flask was cooled in an ice bath and benzene (5 mL, distilled) was added *via* syringe. This was followed by the similar addition of a solution of phosphorus oxychloride ($POCl_3$, distilled, 1.33 mmol, 0.124 mL) in benzene (5 mL). Precipitation of a white solid was observed. More benzene (5 mL) was added and the reaction mixture was allowed to come to room temperature gradually. After standing for 2 days, the vessel was opened carefully (release of pressure was apparent). CH_3OH was added to dissolve the solids and the reaction mixture was then transferred to a round-bottom flask. Benzene and CH_3OH were removed at reduced pressure, and then minimal CH_3OH (*ca.* 6 mL) was added to the flask. After swirling, the supernatant was removed from the remaining solids (51 mg). Concentration provided a white powder (293 mg) which was used without further purification. The final product mixture contained [^{15}N]phosphoric triamide (**7**), [^{15}N]phosphorodiamidic acid (**6**), and $^{15}NH_4Cl$. ^{31}P NMR: [^{15}N]-phosphoric triamide (in H_2O, pH 7) δ = 21.0 ppm (qt, $^1J(^{31}P-^{15}N)$ = 22 Hz); [^{15}N]phosphoric diamide (in H_2O, pH 7) δ = 12.5 ppm (t; $^1J(^{31}P-^{15}N)$ = 16 Hz). ^{15}N NMR: [^{15}N]phosphoric triamide δ = 23.5 ppm (d), [^{15}N]phosphoric diamide δ = 25.9 ppm (doublet).

Note: Attempts to synthesize phosphoric di-, and monoamide by reacting phosphorus oxychloride with 1 or 2 equiv of water followed by excess gaseous ammonia in benzene or tetrahydrofuran were unsuccessful.

NMR Spectroscopy. NMR spectroscopy was performed on a 11.75 T Bruker MSL500 NMR spectrometer. ^{31}P NMR spectroscopy at 202.5 MHz was performed with inverse-gated proton-decoupling over the acquisition time of 0.4 s with a sweep width of 10 000 Hz and a relaxation delay of 1.6 s. ^{13}C NMR spectroscopy at 125.8 MHz was performed with inverse-gated proton decoupling over the acquisition time of 0.5 s with a sweep width of 10 000 Hz and a relaxation delay of 2 s. ^{13}C spectra were referenced to external tetramethylsilane in a coaxial insert. ^{15}N NMR spectra at 50.7 MHz were acquired with inverse-gated proton-decoupling or without decoupling. A sweep width of 6500 Hz and 0.5-s acquisition were used with a 1-s repetition time. ^{17}O NMR at 67.8 MHz was performed without decoupling and with a 20 000 Hz sweep width, a 25-ms acquisition time, and 0.2-s repetition time. Samples for ^{15}N and ^{31}P NMR spectroscopy were placed within 10-mm NMR tubes equipped with a coaxial insert containing 0.05 M [^{15}N]urea in 0.1 M sodium phosphate, pH 7.0. ^{31}P spectra were referenced to this external phosphate resonance at 0 ppm. ^{15}N spectra were referenced to the [^{15}N]-urea (99 atom % ^{15}N; Cambridge Isotope Laboratories) resonance set to 56.5 ppm. The ^{17}O resonance was set to the natural abundance ^{17}O water resonance at 0 ppm.

Typically, samples for NMR spectroscopy were dissolved in 0.1 M NaCl with 10% D_2O to a concentration between 10 and 30 mM. The solutions were immediately cooled in an ice–water bath. The pH meter was calibrated at 20 °C; however, all sample readings were performed in the ice–water bath. The pH of the samples were taken before and after the NMR experiment and agreed to within 0.1 pH unit. The pH values used are the average of the two readings and are not corrected for the deuterium concentration or temperature. All NMR experiments were performed at 4 °C with temperature maintained to within ±1 °C using the Bruker variable-temperature control unit.

One-bond $^{15}N-^1H$ coupling constants are negative; one-bond $^{15}N-^{31}P$ coupling constants can be negative or positive. All coupling constant data are measured directly from the NMR spectrum and are presented as absolute values.

Titration curves were fit to the chemical shift data by equations calculated for a single and double ionization[42] using the curve fitting routine of DeltaGraph (DeltaPoint, Inc.). Although the errors in the curve fit to the data were usually less than 0.05 pH units (see figure legends), the pH measurements were done in an ice–water bath (0–4 °C) while NMR spectra were run at 4 °C. This, combined with the accuracy of the pH meter, leads to an estimate of the errors in the pK_a values to approximately 0.05 pH units.

Chloride Ion Determinations. The rate of chloride ion liberation was measured in buffered solutions at 20 °C containing 6 mM unlabeled phosphoramide mustard cyclohexylammonium salt using a chloride ion specific electrode. Different buffers were used between pH 2.6 and 10.6 (citric acid–Na_2HPO_4, up to pH 7.6; Na_2HPO_4 to pH 8.0; glycine–NaOH to pH 10.6). The initial linear rate of chloride ion production at each pH was measured as a function of time ($d[Cl^-]/dt$).

Theoretical Methods. The structures of all O- and N-protonated phosphoramides (structures **5a–d**, **6a,b**, **7a,b**) were optimized at the Hartree–Fock (HF) level of theory using a 6-31G* basis set. The anionic O- and N-protonated phosphoramidic acids (structures **5a,b**) were reoptimized with a much larger 6-311++G** basis set since diffuse basis functions are often required to get accurate structures for anionic systems. Analytic HF vibrational frequencies were calculated at the optimized geometries with the 6-31G* basis set and Mulliken populations were calculated using a 6-31G** basis set. Single-point Møller–Plesset fourth order perturbation theory (MP4) energies were calculated at these optimized geometries using a 6-31G** basis set. Additionally, second-order Møller–Plesset (MP2) energies were calculated with a larger 6-311++G** basis set.

In order to calculate the aqueous solvation energies, we used the polarizable continuum model (PCM) as described by Tomasi[43]

and others[44,45] to calculate the electrostatic solvent–solute interaction energy, ΔG_{elec}. The cavitation free energy term of Sinanoglu[46] was used to calculate the nonelectrostatic portion of the solvation energy, ΔG_{cav}. Briefly, the PCM model involves determining the solvent-accessible surface[47,48] of the solute molecule and then calculating the charges induced at this surface in the surrounding dielectric medium by the charge distribution of the solute molecule. The solute atomic charges were fitted to reproduce the electric potential at the solvent-accessible surface determined from the HF wave function.[49] The charges induced at the surface were then included in the one-electron portion of the HF Hamiltonian and the wave function was reoptimized. New atomic charges were calculated from the reoptimized wave function and the whole procedure was iterated to convergence (typically 8 PCM–HF iterations). Finally, the electrostatic portion of the solvation energy was computed for the final atomic and induced surface charges. All solvation calculations were carried out with a 6-311++G** basis set at the HF/6-31G* geometries.

Acknowledgment. We would like to thank Dr. Lou-Sing Kan of the Division of Biophysics, The Johns Hopkins University School of Hygiene and Public Health, for his help with the chloride ion selective electrode measurements. This work was supported by Public Health Service grants CA51229 (M.P.G.) and CA16783 (O.M.C.), training grant CA09243-14 (E.M.S.-R) from the National Cancer Institute, American Cancer Society Institutional Research Grant #IRG-32 (S.M.L.), and an award from the Korean Institute for Science and Technology (S.M.L.). This work was carried out in part at the Sandia National Laboratory (M.E.C.) under contract from the U.S. Department of Energy and Supported by its Division of Basic Energy Sciences.

Supplementary Material Available: The complete *Z*-matrices for the Hartree–Fock 6-31G* optimized structures shown in Figure 8 (4 pages). Ordering Information is given on any current masthead page.

References

(1) Friedman, O. M.; Myles, A.; Colvin, M. Cyclophosphamide and Related Phosphoramide Mustards. Current Status and Future Prospects. *Adv. Cancer Chemother.* **1979**, *1*, 143–204.
(2) Colvin, M.; Burndrett, R. B.; Kan, M. N. N.; Jardine, I.; Fenselau, C. Alkylating Properties of Phosphoramide Mustard. *Cancer Res.* **1976**, *36*, 1121–6.
(3) Maddock, C. L.; Handler, A. H.; Friedman, O. M.; Foley, G. E.; Farber, S. Primary Evaluation of Alkylating Agent Cyclohexylamine Salt of *N,N*-Bis(2-chloroethyl)phosphorodiamidic acid (NSC 69945; OMF-59) in Experimental Antitumor Assay Systems. *Cancer Chemother. Rep.* **1966**, *50*, 629–38.
(4) Brock, N.; Hohorst, H. J. The Problem of Specificity and Selectivity of Alkylating Cytostatics: Studies on N-2-Chloroethylamido-oxazaphosphorines. *Z. Krebsforsch. Klin. Onkol.* **1977**, *88*, 185–215.
(5) Engle, T. W.; Zon, G.; Egan, W. ^{31}P NMR Investigations of Phosphoramide Mustard: Evaluation of pH Control Over the Rate of Intramolecular Cyclization to an Aziridinium Ion and the Hydrolysis of This Reactive Alkylator. *J. Med. Chem.* **1979**, *22*, 897–9.
(6) Engle, T. W.; Zon, G.; Egan, W. ^{31}P NMR Kinetic Studies of the Intra- and Intermolecular Alkylation Chemistry of Phosphoramide Mustard and Cognate N-Phosphorylated Derivatives of *N,N*-Bis-(2-chloroethyl)amine. *J. Med. Chem.* **1982**, *25*, 1347–57.
(7) Voelcker, G.; Giera, H. P.; Jäger, L.; Hohorst, H. J. Zur Bindung von Cyclophosphamid und Cyclophosphamid-Metaboliten an Serum-Albumin. *Z. Krebsforsch. Klin. Onkol.* **1978**, *91*, 127–42.
(8) Friedman, O. M. Studies of Some Newer Phosphoramide Mustards. *Cancer Chemother. Rep.* **1967**, *51*, 347–57.
(9) The designation of the nitrogens of phosphoramide mustard as N^1 and N^2 is completely arbitrary and used for convenience in this paper and does not conform to IUPAC standards.
(10) Ludeman, S. M.; Shulman-Roskes, E. M.; Gamcsik, M. P.; Hamill, T. G.; Chang, Y. H.; Koo, K. I.; Colvin, O. M. Synthesis of ^{15}N and ^{17}O Labelled Phosphoramide Mustards. *J. Labelled Compd Radiopharm.* **1993**, *33*, 313–26.
(11) Watson, E.; Dea, P.; Chan, K. K. Kinetics of Phosphoramide Mustard Hydrolysis in Aqueous Solution. *J. Pharmaceut. Sci.* **1985**, *74*, 1283–92.
(12) Ulmer, W. Electronic Structure of the Metabolites of Cyclophosphamide. *Int. J. Quantum Chem.* **1981**, *19*, 337–59.
(13) Jaffe, E. K.; Cohn, M. ^{31}P Nuclear Magnetic Resonance Spectra of the Thiophosphate Analogues of Adenine Nucleotides; Effects of pH and Mg^{2+} Binding. *Biochemistry* **1978**, *17*, 652–7.
(14) Gadian, D. G.; Radda, G. K.; Richards, R. E.; Seeley, P. J. In *Biological Applications of Magnetic Resonance*; Shulman, R. G., Eds.; Academic Press: New York, 1979; pp 463–535.
(15) Duthaler, R. O.; Roberts, J. D. Steric and Electronic Effects on ^{15}N Chemical Shifts of Saturated Aliphatic Amines and Their Hydrochlorides. *J. Am. Chem. Soc.* **1978**, *100*, 3889–95.
(16) Kalinowski, H. O.; Berger, S.; Braun, S. *Carbon-13 NMR Spectroscopy*; John Wiley & Sons: New York, 1988; pp 221–231.
(17) Gerothanassis, I. P.; Sheppard, N. Natural-Abundance ^{17}O NMR Spectra of Some Inorganic and Biologically Important Phosphates. *J. Magn. Reson.* **1982**, *46*, 423–39.
(18) Gerlt, J. A.; Demou, P. C.; Mehdi, S. ^{17}O NMR Spectral Properties of Simple Phosphate Esters and Adenine Nucleotides. *J. Am. Chem. Soc.* **1982**, *104*, 2848–56.
(19) Gerlt, J. A.; Reynolds, M. A.; Demou, P. C.; Kenyon, G. L. ^{17}O NMR Spectral Properties of Pyrophosphate, Simple Phosphonates, and Thiophosphate and Phosphonate Analogues of ATP. *J. Am. Chem. Soc.* **1983**, *105*, 6469–74.
(20) Reynolds, M. A.; Gerlt, J. A.; Demou, P. C.; Oppenheimer, N. J.; Kenyon, G. L. ^{15}N and ^{17}O NMR Studies of the Proton Binding Sites in Imidodiphosphate, Tetraethyl Imido-diphosphate, and Adenylyl Imidodiphosphate. *J. Am. Chem. Soc.* **1983**, *105*, 6475–81.
(21) Hunston, R. N.; Gerothanassis, I. P.; Lauterwein, J. A Study of L-Proline, Sarcosine, and the Cis/Trans Isomers of *N*-Acetyl-L-Proline and *N*-Acetylsarcosine in Aqueous and Organic Solution by ^{17}O NMR. *J. Am. Chem. Soc.* **1985**, *107*, 2654–61.
(22) Emsley, J.; Hall, D. *The Chemistry of Phosphorus*; John Wiley & Sons: New York, 1976; pp 381–383.
(23) Rahil, J.; Haake, P. Reactivity and Mechanism of Hydrolysis of Phosphonamides. *J. Am. Chem. Soc.* **1981**, *103*, 1723–34.
(24) Levine, D.; Wilson, I. B. The Dipolar Ion Structure of Phosphoramidic Acid. Heats of Ionization. *Inorg. Chem.* **1968**, *7*, 818–20.
(25) Jencks, W. P.; Gilchrist, M. Electrophilic Catalysis. The Hydrolysis of Phosphoramidic acid. *J. Am. Chem. Soc.* **1964**, *86*, 1410–17.
(26) Hobbs, E.; Corbridge, D. E. C.; Raistrick, B. The Crystal Structure of *Monosodium* Phosphoramidate $NaHPO_3NH_2$. *Acta Crystallogr.* **6**, 621 (1953).
(27) Crunden, E. W.; Hudson, R. F. The Mechanism of Hydrolysis of Phosphorochloridates and Related Compounds. Part III. Phosphoramidochloridates. *J. Chem. Soc.* **1962**, 3591–9.
(28) Bollinger, J. C.; Houriet, R.; Kern, C. W.; Perret, D.; Weber, J.; Yvernault, T. Experimental and Theoretical Studies of the Gas-Phase Protonation of Aliphatic Phosphine Oxides and Phosphoramides. *J. Am. Chem. Soc.* **1985**, *107*, 5352–8.
(29) Modro, T. A.; Liauw, W. G.; Peterson, M. R.; Csizmadia, I. G. Protonation of Phosphoric Amide. Molecular Orbital Calculations on Phosphinamide, $H_2P(O)NH_2$, and Its Protonated Forms. *J. Chem. Soc. Perkin 2* **1979**, 1432–6.
(30) Allen, F. H.; Kennard, O.; Watson, D. G.; Brammer, L.; Orpen, A. G.; Taylor, R. Tables of Bond Lengths Determined by X-Ray and Neutron Diffraction. Part 1. Bond Lengths in Organic Compounds. *J. Chem. Soc. Perkin Trans. II* **1987**, S1–S19.
(31) Locke, M. J.; McIver, R. T., Jr. Effect of Solvation on the Acid/Base Properties of Glycine. *J. Am. Chem. Soc.* **1983**, *105*, 4226–32.
(32) Locke, M. J.; Hunter, R. L.; McIver, R. T., Jr., Experimental Determination of the Acidity and Basicity of Glycine in the Gas Phase. *J. Am. Chem. Soc.* **1979**, *101*, 272–3.
(33) Still, W. C.; Tempczyk, A.; Hawley, R. C.; Hendrickson, T. Semianalytical Treatment of Solvation for Molecular Mechanics and Dynamics. *J. Am. Chem. Soc.* **1990**, *112*, 6127–9.
(34) Cramer, C. J.; Truhlar, D. G. General Parameterized SCF Model for Free Energies of Solvation in Aqueous Solution. *J. Am. Chem. Soc.* **1991**, *113*, 8305–11.
(35) Cramer, C. J.; Truhlar, D. G. An SCF Solvation Model for the Hydrophobic Effect and Absolute Free Energies of Aqueous Solvation. *Science* **1992**, *256*, 213–7.
(36) Colvin, M. E.; Melius, C. F.; Ludeman, S. M.; Colvin, O. M.; Gamcsik, M. P.; Hausheer, F. H. Unpublished results.
(37) Boal, J. H.; Williamson, M.; Boyd, V. L.; Ludeman, S. M.; Egan, W. ^{31}P NMR Studies of the Kinetics of Bisalkylation by Isophosphoramide Mustard: Comparisons with Phosphoramide Mustard. *J. Med. Chem.* **1989**, *32*, 1768–73.
(38) Golding, B. T.; Kebell, M. J.; Lockhart, I. M. Chemistry of Nitrogen Mustard (2-Chloro-N-(2-chloroethyl)-N-methylethanamine) Studied by Nuclear Magnetic Resonance Spectroscopy. *J. Chem. Soc. Perkin Trans. 2* **1987**, 705–713.
(39) Gamcsik, M. P.; Hamill, T. G.; Colvin, M. NMR Studies of the Conjugation of Mechlorethamine with Glutathione. *J. Med. Chem.* **1990**, *33*, 1009–14.

(40) Gamcsik, M. P.; Millis, K. K.; Ludeman, S. M.; Shulman-Roskes, E. M.; Hausheer, F. H.; Colvin, O. M. Unpublished results.
(41) Cohen, B.; van Artsdalen, E. R.; Harris, J. Reaction Kinetics of Aliphatic Tertiary β-Chloroethylamines in Dilute Aqueous Solution. I. The Cyclization Process. *J. Am. Chem. Soc.* **1948**, *70*, 281–5.
(42) Malthouse, J. P. G.; Primrose, W. U.; Mackenzie, N. E.; Scott, A. I. ^{13}C NMR Study of the Ionizations within a Trypsin-Chloromethyl Ketone Inhibitor Complex. *Biochemistry* **1985**, *24*, 3478–87.
(43) Miertus, S.; Scrocco, E.; Tomasi, J. Electrostatic Interaction of a Solute with a Continuum. A Direct Utilization of *Ab Initio* Molecular Potentials for the Prevision of Solvent Effects. *Chem. Phys.* **1981**, *55*, 117–29.
(44) Rashin, A. A.; Namboodiri, K. A Simple Method for the Calculation of Hydration Enthalpies of Polar Molecules with Arbitrary Shapes. *J. Phys. Chem.* **1987**, *91*, 6003–12.
(45) Zauhar, R. J.; Morgan, R. S. A New Method for Computing the Macromolecular Electric Potential. *J. Mol. Biol.* **1985**, *186*, 815–20.
(46) Halcioglu, T.; Sinanoglu, O. Solvents Effects on Cis-Trans Azobenzene Isomerization: A Detailed Application of a Theory of Solvent Effects on Molecular Association. *Ann. N.Y. Acad. Sci.* **1969**, *158*, 308–317.
(47) Zauhar, R. J.; Morgan, R. S. Computing the Electric Potential of Biomolecules: Application of a New Method of Molecular Surface Triangulation. *J. Comput. Chem.* **1990**, *11*, 603–22.
(48) Connolly, M. L. Solvent-Accessible Surfaces of Proteins and Nucleic Acids. *Science* **1983**, *221*, 709–13.
(49) Colvin, M. E.; Melius, C. F. Continuum Solvent Models for Computational Chemistry. *Sandia National Laboratories*, **1993**, 1–34.
(50) Bachovchin, W. W.; Roberts, J. D. N-15 NMR Spectroscopy. The State of Histidine in the Catalytic Triad of α-Lytic Protease. Implications for the Charge Relay Mechanism of Peptide Bond Cleavage. *J. Am. Chem. Soc.* **1978**, *100*, 8041–7.
(51) Blomberg, F.; Maurer, W.; Rüterjans, H. Nuclear Magnetic Resonance Investigation of ^{15}N-Labeled Histidine in Aqueous Solution. *J. Am. Chem. Soc.* **1977**, *99*, 8149–59.